Measuring the Weizsäcker-Williams distribution of linearly polarized gluons at an electron-ion collider through dijet azimuthal asymmetries

Vladimir Skokov[*][†]

Department of Physics, North Carolina State University, Raleigh, North Carolina 27695, USA
RIKEN-BNL Research Center, Brookhaven National Laboratory, Upton, New York 11973-5000, USA
E-mail: VSkokov@ncsu.edu

The Weizsäcker-Williams transverse momentum dependent (TMD) gluon distributions can be probed in the production of a hard dijet in semi-inclusive DIS. This process is sensitive not only to the conventional but also to the linearly polarized gluon distribution. The latter gives rise to an azimuthal dependence of the dijet cross section and therefore can be distinguished from the former. Feasibility study of a measurement of these TMDs through dijet production at a future electron-ion collider shows that the extraction of the distribution of linearly polarized gluons with a statistical accuracy of 5% will require estimated luminosity of 20 fb^{-1}/A.

XXVII International Workshop on Deep-Inelastic Scattering and Related Subjects - DIS2019
8-12 April, 2019
Torino, Italy

---

[*]Speaker.

1. Introduction

In this proceedings, I summarize the fundings of Ref. [1], where the conventional and linearly polarized Weizsäcker-Williams (WW) gluon distributions at small x [2, 3, 4] were studied with the goal of accessing the feasibility of a measurement of the gluon distributions at an EIC through the dijet production process.

At leading order in α_s and in the small-x, high-energy limit, to leading power in the inverse dijet total transverse momentum, the cross-section for inclusivexproduction of a $q + \bar{q}$ dijet in high energy deep inelastic scattering of a virtual photon γ^* off a proton or nucleus is given by [3, 5]

$$E_1 E_2 \frac{d\sigma^{\gamma_T^* A \rightarrow q\bar{q}X}}{d^3 k_1 d^3 k_2 d^2 b} = \alpha_{em} e_q^2 \alpha_s \delta\left(1 - z - \bar{z}\right) z\bar{z} \left(z^2 + \bar{z}^2\right) \frac{\varepsilon_f^4 + P_\perp^4}{(P_\perp^2 + \varepsilon_f^2)^4}$$

$$\times \left[xG^{(1)}(x, q_\perp) - \frac{2\varepsilon_f^2 P_\perp^2}{\varepsilon_f^4 + P_\perp^4} \cos(2\phi) \, xh_\perp^{(1)}(x, q_\perp) \right] , \quad (1.1)$$

$$E_1 E_2 \frac{d\sigma^{\gamma_L^* A \rightarrow q\bar{q}X}}{d^3 k_1 d^3 k_2 d^2 b} = \alpha_{em} e_q^2 \alpha_s \delta\left(1 - z - \bar{z}\right) z^2 \bar{z}^2 \frac{8\varepsilon_f^2 P_\perp^2}{(P_\perp^2 + \varepsilon_f^2)^4}$$

$$\times \left[xG^{(1)}(x, q_\perp) + \cos(2\phi) \, xh_\perp^{(1)}(x, q_\perp) \right] , \quad (1.2)$$

where b is the impact parameter. The transverse momenta (light-cone momentum fractions) of the produced quark and anti-quark are given by $\vec{k}_{1\perp}$ (z) and $\vec{k}_{2\perp}$ ($\bar{z}$). These quantities can be combined into the dijet total transverse momentum $\vec{P}_\perp$ and the momentum imbalance $\vec{q}_\perp$:

$$\vec{P}_\perp = \bar{z}\vec{k}_{1\perp} - z\vec{k}_{2\perp} \ , \ \ \vec{q}_\perp = \vec{k}_{1\perp} + \vec{k}_{2\perp} . \quad (1.3)$$

The angle ϕ denotes the azimuthal angle between $\vec{P}_\perp$ and $\vec{q}_\perp$. Only the case when $\vec{P}_\perp$ is greater than $\vec{q}_\perp$, also known as the "correlation limit", is considered here. Power corrections to Eqs. (1.1,1.2) generate additional contributions $\sim (Q_s^2/P_\perp^2) \log P_\perp$ to the isotropic and $\sim \cos 2\phi$ terms [6]. Also, a $\cos 4\phi$ angular dependence arises from power corrections of order $q_\perp^2/P_\perp^2$. Although these corrections might be important for phenomenology at an EIC, they are neglected in the present summary.

The average $\cos 2\phi$ measures the azimuthal anisotropy, $v_2 \equiv \langle \cos 2\phi \rangle$, where averaging is performed over ϕ at fixed $q_\perp$ and $P_\perp$, with normalized weights proportional to the respective cross-sections.

The gluon x,

$$x = \frac{1}{W^2 + Q^2 - M^2} \left(Q^2 + q_\perp^2 + \frac{1}{z\bar{z}} P_\perp^2 \right) , \quad (1.4)$$

is independent of ϕ and, therefore, for definite polarization of the virtual photon we obtain [7]

$$v_2^L = \frac{1}{2} \frac{xh_\perp^{(1)}(x, q_\perp)}{xG^{(1)}(x, q_\perp)} \ , \ \ v_2^T = -\frac{\varepsilon_f^2 P_\perp^2}{\varepsilon_f^4 + P_\perp^4} \frac{xh_\perp^{(1)}(x, q_\perp)}{xG^{(1)}(x, q_\perp)} . \quad (1.5)$$

In experiments it is not possible to distinguish the polarization of the photon in dijet production. Nevertheless, as will be shown at the end of this proceedings, a careful analysis of experimental data may give access to contributions from different polarizations.
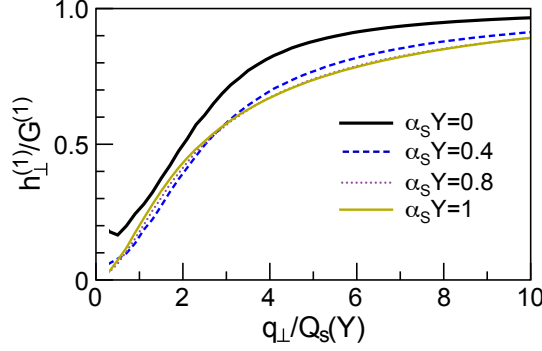
1

Figure 1: $xG^{(1)}(x,q_\perp^2)$ and $xh^{(1)}(x,q_\perp^2)$ versus transverse momentum $q_\perp$ at different rapidities $Y = \log x_0/x$. $Q_s(Y)$ is the saturation momentum.

An important phenomenological difference between the conventional and linearly polarized distribution is that the former can also be measured in $\gamma A \to q\bar{q}X$ in the $Q^2 \to 0$ limit, while for a real photon $\varepsilon_f^2 \propto Q^2 \to 0$ the cross-section for the dijet production becomes isotropic and no longer useful for extracting $xh_\perp^{(1)}(x,q_\perp^2)$.

Numerical solutions of the JIMWLK evolution equation to small x were presented in Ref. [7], shown in Fig. 1. At small transverse momentum, the polarization is significantly suppressed. At $q_\perp \gg Q_s(Y)$, $xh^{(1)}(x,q_\perp^2) \to xG^{(1)}(x,q_\perp^2)$ corresponding to maximal polarization. For the momentum imbalance of order the saturation momentum, these numerical simulations show a substantial angular modulation of the dijet cross-section, because $xh^{(1)}(x,q_\perp^2)/xG^{(1)}(x,q_\perp^2) \simeq 10\% - 20\%$.

To simulate $q + \bar{q}$ dijet production, described by Eqs. (1.1) or (1.2), a Monte-Carlo code (MCDijet) was developed in Ref. [1]. For details on the implementation, we refer the reader to Ref. [1], instead we turn to practical application of MCDijet to an EIC.

2. Feasibility studies

In order to show that the anisotropy generated on $q + \bar{q}$ level is not lost during reconstruction of dijets within restrictions of a realistic detector environment and to estimate that the DIS background processes can be suppressed sufficiently by kinematic cuts not to affect the level of anisotropy, we performed the analysis of pseudo-data generated by the Monte Carlo generator MCDijet, PYTHIA 8.2 [8] for showering of partons generated by MCDijet, and PYTHIA 6.4 [9] for background studies. Jets are reconstructed with the FastJet package [10].

Figure 2 shows the resulting $d\sigma/d\phi$ distributions for the original parton pairs and the reconstructed dijets in $\sqrt{s}$=90 GeV e+Au collisions for $1.25 < q_\perp < 1.75$ GeV/c and $3.00 < P_\perp < 3.50$ GeV/c. The results are based on 10M generated events but the error bars were scaled to reflect an integrated luminosity of 10 fb^{-1}/nucleon. The plot a) shows the azimuthal anisotropy for all virtual photon polarizations, and plots b) and c) for transversal and longitudinal polarized photons, respectively. The quantitative measure of the anisotropy, v_2, is listed in the figures. The values shown are those for parton pairs; the accompanying numbers in parenthesis denote the values derived from
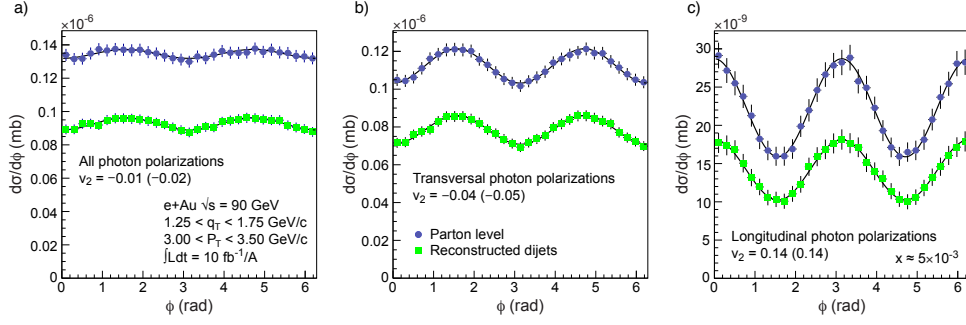
Figure 2: $d\sigma/d\phi$ distributions for parton pairs (circles) generated with the MCDijet generator and corresponding reconstructed dijets (squares) in $\sqrt{s}$=90 GeV e+A collisions for $1.25 < q_\perp < 1.75$ GeV/c and $3.00 < P_\perp < 3.50$ GeV/c. The error bars reflect an integrated luminosity of 10 fb^{-1}/nucleon.

the reconstructed dijets. The reconstructed dijets reflect the original anisotropy at the parton level rather well. The loss in dijet yield is mostly due to low-p_T particles and is on the order of 25%.

While MCDijet provides a tool to study the signal anisotropy in great detail it does neither generate complete events, nor does it allow us to derive the level of false identification of dijets in events unrelated to dijet production. The purity of the extracted signal sample ultimately determines if these measurements can be conducted. For studies of this kind we have to turn to PYTHIA6, an event generator that includes a relatively complete set of DIS processes.

Most of the measurements with dijets in $e + p$ collisions at HERA (see for example [11, 12]) were carried out at high Q^2 and high jet energies ($E_{\text{jet}} > 10$ GeV). Here, however, we focus on moderately low virtualities and relatively small jet transverse momenta $P_\perp$. As a result, the dijet signal is easily contaminated by beam remnants. To minimize this background source we limit jet reconstruction to $1 < \eta < 2.5$, sufficiently far away from the beam fragmentation region.
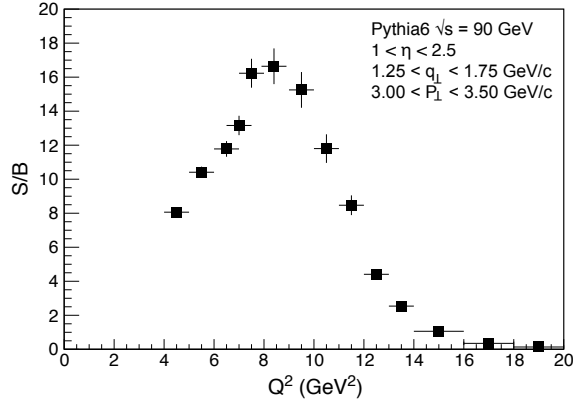

Figure 3: Q^2 dependence of the signal-to-background ratio derived from PYTHIA6.

In PYTHIA6 study, we count $f_i + \gamma^*_{\text{T,L}} \to f_i + g$ and $g + \gamma^*_{\text{T,L}} \to f_i + \bar{f}_i$ as signal and all other as background processes. The dominant background source is the standard LO DIS process $\gamma^* + q \to q$. Figure 3 illustrates the Q^2 dependence of the signal-to-background ratio, *i.e.*, the number of correctly reconstructed signal events over the number of events that were incorrectly flagged as containing a signal dijet process. The signal-to-background ratio rises initially due to the improved

dijet reconstruction efficiency towards larger Q^2 (or $P_\perp$) but then drops dramatically as particles from the beam remnant increasingly affect the jet finding. In what follows, we limit our study to $4 \le Q^2 \le 12 \text{ GeV}^2$.

In order to derive the distribution of linearly polarized gluons via Eqs. (1.5), the contributions from transverse (v_2^T) and longitudinally polarized photons (v_2^L) need to be disentangled. With the exception of diffractive J/ψ production, no processes in DIS exist where the polarization of the virtual photon can be measured directly. In our case there are three features that do make the separation possible: v_2^L and v_2^T have opposite signs (see Fig. 2), the background contribution shows no anisotropy, and the existence of the relation

$$v_2^{\text{unpol}} = \frac{Rv_2^L + v_2^T}{1+R}, \qquad R = \frac{8\varepsilon_f^2 P_\perp^2 \, z(1-z)}{(z^2 + (1-z)^2)\,(\varepsilon_f^4 + P_\perp^4)}. \qquad (2.1)$$
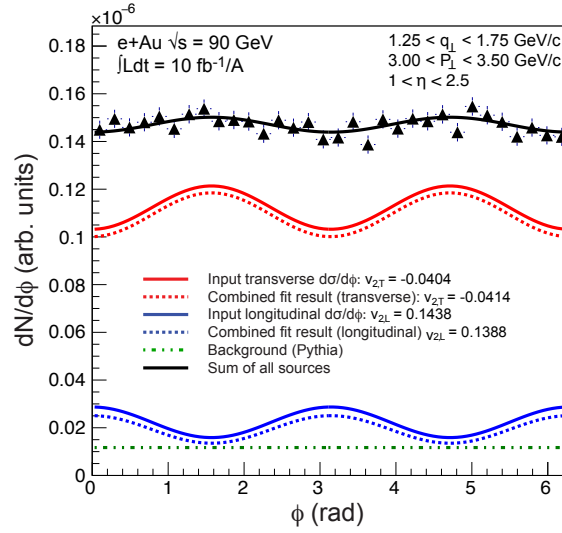

Figure 4: Result of a fit of combined signal and background to a data sample obtained in $\sqrt{s} = 90$ GeV e+A collisions with an integrated luminosity of 10 fb^{-1}/nucleon.

Our strategy is to perform a combined 5-parameter fit of all 3 components to the full data sample: The signal for longitudinal polarization (σ_L, v_2^L), that for transverse polarization (σ_T, v_2^T), and the flat background (σ_b). We generated the data sample in a separate Monte-Carlo combining the signal from MCDijet with the background contribution from PYTHIA6 while smearing each data point randomly according to the statistics available at a given integrated luminosity. The fit provides the desired v_2^L and v_2^T.

Figure 4 shows the result of one typical fit on data generated for a integrated luminosity of 10 fb^1/nucleon. The scatter and errors on the data points reflect the size of the potential data sample, the red and the blue curves illustrate the input (solid curve) and the fit result (dashed curve) for v_2^L and v_2^T. The dashed curves were offset for better visibility.

Additionally systematic studies not presented here showed that the relative errors improve with increasing $P_\perp$, *i.e.*, increasing v_2. Our results indicate that a proper measurement of the linearly polarized gluon distribution will require integrated luminosities of at least 20 fb^{-1}/nucleon or more.

3. Conclusion

Monte-Carlo simulations with restrictions of a realistic detector environment show that it is feasible to study the Weizsäcker-Williams transverse momentum dependent (TMD) gluon distributions, in particular, linearly polarized distribution, at an electron-ion collider. This, however, might require a multi-year program assuming that an initial EIC luminosity is around 10^{33} cm^{-2} s^{-1}, as a proper measurement of the linearly polarized gluon distribution demands integrated luminosities of at least 20 fb^{-1}/nucleon or more.

4. Acknowledgement

References

[1] A. Dumitru, V. Skokov and T. Ullrich, Phys. Rev. C **99**, no. 1, 015204 (2019) doi:10.1103/PhysRevC.99.015204 [arXiv:1809.02615 [hep-ph]].

[2] D. Boer, S. J. Brodsky, P. J. Mulders and C. Pisano, Phys. Rev. Lett. **106**, 132001 (2011) doi:10.1103/PhysRevLett.106.132001 [arXiv:1011.4225 [hep-ph]].

[3] F. Dominguez, C. Marquet, B. W. Xiao and F. Yuan, Phys. Rev. D **83**, 105005 (2011) doi:10.1103/PhysRevD.83.105005 [arXiv:1101.0715 [hep-ph]].

[4] F. Dominguez, J. W. Qiu, B. W. Xiao and F. Yuan, Phys. Rev. D **85**, 045003 (2012) doi:10.1103/PhysRevD.85.045003 [arXiv:1109.6293 [hep-ph]].

[5] A. Metz and J. Zhou, Phys. Rev. D **84**, 051503 (2011) doi:10.1103/PhysRevD.84.051503 [arXiv:1105.1991 [hep-ph]].

[6] A. Dumitru and V. Skokov, Phys. Rev. D **94**, no. 1, 014030 (2016) doi:10.1103/PhysRevD.94.014030 [arXiv:1605.02739 [hep-ph]].

[7] A. Dumitru, T. Lappi and V. Skokov, Phys. Rev. Lett. **115**, no. 25, 252301 (2015) doi:10.1103/PhysRevLett.115.252301 [arXiv:1508.04438 [hep-ph]].

[8] T. Sjöstrand *et al.*, Comput. Phys. Commun. **191**, 159 (2015) doi:10.1016/j.cpc.2015.01.024 [arXiv:1410.3012 [hep-ph]].

[9] T. Sjostrand, S. Mrenna and P. Z. Skands, JHEP **0605**, 026 (2006) doi:10.1088/1126-6708/2006/05/026 [hep-ph/0603175].

[10] M. Cacciari, G. P. Salam and G. Soyez, Eur. Phys. J. C **72**, 1896 (2012) doi:10.1140/epjc/s10052-012-1896-2 [arXiv:1111.6097 [hep-ph]].

[11] A. Aktas *et al.* [H1 Collaboration], JHEP **0710**, 042 (2007) doi:10.1088/1126-6708/2007/10/042 [arXiv:0708.3217 [hep-ex]].

[12] M. Gouzevitch [H1 and ZEUS Collaborations], J. Phys. Conf. Ser. **110**, 022015 (2008). doi:10.1088/1742-6596/110/2/022015